

COLOR GLASS CONDENSATE IN QCD AT HIGH ENERGY

KAZUNORI ITAKURA

Service de Physique Théorique, CEA/Saclay, F-91191, Gif-sur-Yvette, France

E-mail: itakura@spht.saclay.cea.fr

I give a brief review about the color glass condensate, which is the universal form of hadrons and nuclei at high energies.

1 The Color Glass Condensate

The main purpose of this talk is to convince you that *high energy limit of QCD is the Color Glass Condensate*.¹ More precisely, when the energy of hadronic scattering is very large, the participating hadrons or nuclei behave not as usual states made of valence particles, but as new form of matter called the color glass condensate (CGC). This name is after the following observations. First of all, it is made of gluons ("small- x gluons") which have **color** and carry small fractions $x \ll 1$ of the total momentum. Next, these small- x gluons are created by slowly moving color sources (partons with larger x) which are distributed randomly on the two dimensional disk (the Lorentz contracted hadron). This is like a **glass** whose constituents are disordered and appear to be frozen in short time scales. Lastly, the density of small- x gluons becomes very large until it is saturated to some value. Typically the occupation number of gluons is of $\mathcal{O}(1/\alpha_s) \gg 1$ at saturation, which is like a **condensate** of bosons. As the scattering energy is increased, the hadrons undergo multiple production of small- x gluons, and eventually become the CGC.

Note that the claim above is as correct as the statement about the other limits of QCD: high temperature/density limit of QCD is the QGP/color superconductor, which now everyone believes true. In the same sense, if one goes to high energy limit in QCD, one will necessarily encounter the CGC. Note also that these three different limits allow for weak-coupling descriptions powered by sophisticated resummation schemes.

2 Gluon saturation and unitarity

Let us explain how the CGC appears with increasing energy. When the gluon density is not so high, change of the gluon distribution with increasing energy (or decreasing x) is described by the BFKL evolution equation:²

$$\frac{\partial}{\partial \tau} \mathcal{N}_\tau(k) = \bar{\alpha}_s K_{\text{BFKL}} \otimes \mathcal{N}_\tau(k), \quad (1)$$

where $\bar{\alpha}_s = \alpha_s N_c / \pi$, $\mathcal{N}_\tau(k)$ is the dipole-proton scattering amplitude (or unintegrated gluon distribution of the target proton), $\tau = \ln 1/x$ is the rapidity, and $\bar{\alpha}_s K_{\text{BFKL}}$ is the kernel representing the probability of splitting of one dipole into two. This is essentially a linear differential equation, and its solution at asymptotically large energies shows exponential growth of $\mathcal{N}_\tau(k)$. Namely, multiple production of gluons occurs endlessly. This, however, violates the unitarity bound for the cross section (or, $\mathcal{N}_\tau \leq 1$) and the BFKL equation must be modified so as not to violate the unitarity. In fact, what is missing in the BFKL equation is the *recombination process* of two gluons into one, which cannot be ignored when the gluon density is high. Note that this process effectively reduces the speed of growth. Once this is included, the BFKL equation is replaced by the Balitsky-Kovchegov (BK) equation:³

$$\frac{\partial}{\partial \tau} \mathcal{N}_\tau(k) = \bar{\alpha}_s K_{\text{BFKL}} \otimes (\mathcal{N}_\tau(k) - \mathcal{N}_\tau^2(k)). \quad (2)$$

Compared to the BFKL solution, the solution to this equation is drastically changed due to the presence of the nonlinear term. Indeed, it exhibits saturation (unitarization) of the amplitude and a kind of universality, as I will explain below in a simple example.

2.1 Analogy with population growth

In order to understand what happens in the BK equation, let us ignore the transverse dynamics for the time being. This simplification allows us to find an interesting analogy with the problem of population growth. Long time ago, Malthus discussed that growth rate of population should be proportional to the population itself, and proposed a simple linear equation for the population density $N(t)$:

$$\frac{d}{dt}N(t) = \alpha N(t). \quad (3)$$

Its solution $N(t) = N_0 e^{\alpha t}$ shows exponential growth known as the "population explosion." However, as the number of people increases, this equation fails to describe the actual growth. This is because various effects such as lack of foods reduce the speed of growth. One can effectively represent such effects by replacing the growth constant α by $\alpha(1 - N)$ which decreases with increasing N . This yields the famous *logistic equation* first proposed by Verhulst:

$$\frac{d}{dt}N(t) = \alpha (N(t) - N^2(t)). \quad (4)$$

This *nonlinear* equation can be solved analytically. The similarity of these equations to our problem is rather trivial: N and t correspond to the scattering amplitude and the rapidity, respectively. In Fig. 1, we show the solutions to eq. (4) with different initial conditions at $t = 0$, together with the corresponding solutions to the linear equation (3). We can learn much from this result. First of all, at early time $t \sim 0$, the solution shows exponential growth as in the linear case. However, as $N(t)$ grows, the nonlinear term ($\sim N^2$) becomes equally important, and the speed of growth is reduced. Eventually at late time, the solution approaches a constant which is determined by the asymptotic condition $dN/dt = 0$. This corresponds to the *saturation* and *unitarization* of the gluon number. Next, note that two solutions of the logistic equation with different initial conditions approach to each other, and converge to the

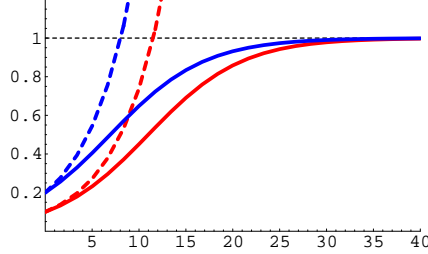


Figure 1. Solutions to eq. (4) [solid lines] and eq. (3) [dashed lines], with different initial conditions.

same value, while deviation of two solutions of the linear equation expands as time goes. Namely, in the logistic equation, the initial condition dependence disappears as $t \rightarrow \infty$, which is related to the *universality* of the BK equation. This analogy may look oversimplified, but actually most of the phenomena seen in the BK equation can be identified in this simple example, as far as energy dependence of the solution is concerned.^a

3 Saturation scale

Let us turn to the transverse dynamics which was ignored above. The most important quantity associated with the transverse dynamics is the *saturation scale* Q_s , which gives the border line between the saturated (non-linear) and non-saturated (linear) regimes. Physically, it corresponds to (inverse of) the typical transverse size of gluons when the transverse plane of a hadron or nucleus is filled with gluons. More precisely, it is given by the scale Q^2 satisfying

$$\sigma \cdot \rho = 1, \text{ with } \sigma = \frac{\alpha_s}{Q^2}, \quad \rho = \frac{xG(x, Q^2)}{\pi R^2}. \quad (5)$$

Here σ is the cross section between the external probe and a gluon, and ρ is the gluon density per unit transverse area of the target with its radius R . Note that the saturation scale depends upon both x and atomic number A . Its x and A dependences can be precisely determined by the BK equation or the linear BFKL equation with saturation

^aIndeed, the logistic equation (4) is obtained in the homogeneous approximation of the FKPP equation, which is essentially equivalent to the BK equation.⁴

boundary condition. When x is not too small, one finds^{5,6,7,8}

$$Q_s^2(x, A) \propto A^{1/3} x^{-\lambda} \quad (6)$$

where λ is given by $4.88\bar{\alpha}_s$ from the LO-BFKL, and $\lambda \sim 0.3$ for $x = 10^{-2} - 10^{-4}$ from (resummed) NLO-BFKL. Also, for the running coupling case, A dependence of Q_s disappears at very large energy (small x).⁹ This particular dependence upon x and A leads to an interesting observation that the saturation scales for the deep inelastic scattering (DIS) at HERA and for the Au-Au collisions at RHIC are of the same order. Therefore, if one finds saturation effects in the HERA data, then there is enough reason to expect similar things in the RHIC data.

4 Geometric scaling

Geometric scaling¹⁰ is one of the most significant experimental facts which provides an indirect evidence of the CGC. This is a new scaling phenomenon at small x meaning that the total γ^* -proton cross section $\sigma_{\text{total}}^{\gamma^*p}$ in DIS depends upon Q^2 and x only via their specific combination $\xi \equiv Q^2 R_0^2(x)$, with $R_0^2(x) \propto x^\lambda$, $\lambda \sim 0.3$. Recall that $1/Q$ is the transverse size of gluons measured by the virtual photon, and, particularly, $1/Q_s$ is the gluon size when the transverse plane of the proton is filled with gluons. Therefore, if we identify $R_0(x) \equiv 1/Q_s(x)$, then the scaling variable ξ^{-1} turns out to be a ratio between the transverse areas of these gluons $\xi^{-1} = \sigma_g/\sigma_{\text{sat}}$. Moreover, if gluons are distributed homogeneously over the transverse plane, which is realized in the saturated regime, ξ^{-1} corresponds to the *number of covering times*. For example, when $\xi = 1$, the transverse plane is covered by gluons *once* which, however, can be realized by various size of gluons. Since what matters in the saturated regime is the effective number of overlapping, it is natural that different kinematics can give the same value of cross section if the number of covering is the same. This is nothing but the geometric scaling! Furthermore, it is remarkable that the theoretical calculation for the x de-

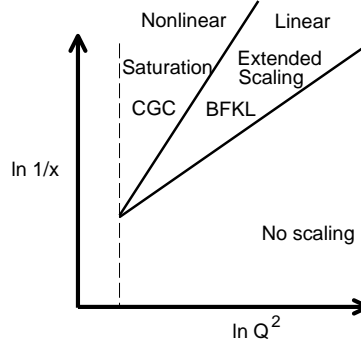


Figure 2. "Phase diagram" of a proton in DIS.

pendence of $Q_s(x)$ is consistent with the experimentally determined one $Q_s^2(x) \propto x^{-0.3}$.

The scenario discussed so far holds naturally in the saturation regime. On the other hand, the data show the geometric scaling up to higher values of Q^2 ($\sim 100 \text{ GeV}^2$), which is the non-saturated regime described by the linear BFKL equation. Indeed, this is again well understood in the context of CGC. The geometric scaling appears if one solves the BFKL equation *with a saturation boundary condition*. As we depart from the saturation line toward the linear regime, the effect of saturation becomes weaker and weaker and eventually disappears. In fact, one can determine the window for the geometric scaling:⁶

$$Q_s^2(x) \lesssim Q^2 \lesssim Q_s^4(x)/\Lambda_{\text{QCD}}^2 \quad (7)$$

Hence we recognized that there is a qualitatively different regime in between the CGC and DGLAP regimes, as is shown in Fig. 2.

5 The CGC confronts experiments

Our understanding of the CGC has been developed with the experimental results at HERA and RHIC, as we already saw above. Below I briefly explain some of the attempts to describe/understand the other experimental data from the viewpoint of CGC.

5.1 HERA small x data

DIS at small x is the cleanest process for measuring the saturation effects in gluon distribution of the proton. Starting from the pioneering work by Golec-Biernat and Wüsthoff,¹² there are several efforts to describe the HERA

DIS data such as the F_2 structure function at small x , in the context of gluon saturation. Here let us explain the "CGC fit"¹³ which is one of the most successful fits of the small x data based on QCD. The CGC fit is constructed so as to contain two approximate solutions to the BK equation, which are valid in the saturation and BFKL regimes, respectively. In particular, the solution in the linear BFKL regime shows the geometric scaling and its (small) violation. With only three parameters, the CGC fit provides a very nice fit for the F_2 structure function with $x < 10^{-2}$ and in $0.045 < Q^2 < 45 \text{ GeV}^2$. Meanwhile, it turned out that this fit works reasonably well even for other observables such as F_2^{diff} and the vector meson production.

5.2 RHIC Au-Au data

The CGC provides the initial condition for the heavy ion collision. Information of the initial state could still be seen in the final observed data. It should be noticed that most of the produced particles have small momenta less than 1 GeV which is of the same order as Q_s in RHIC. This observation suggests that effects of saturation may be visible in bulk quantities such as the multiplicity. Indeed, the CGC results¹¹ for the pseudo-rapidity and centrality dependences of the multiplicity are in good agreement with the data.

5.3 RHIC d-Au data

The CGC has recently come under the spotlight with the experimental results¹⁴ for the nuclear modification factor in the deuteron-Au collisions measured by the Brahm experiment at RHIC. The data show enhancement of the ratio at mid-rapidity (the Cronin effect) and suppression at forward rapidities. In fact, the global behavior of the data is qualitatively consistent with the predictions made by the CGC.^{15,16} More recently, detailed analysis of the ratio was done¹⁷ and it has been clarified that the Cronin effect is due to the multiple collision and re-distribution of the gluons which is properly described by

the McLerran-Venugopalan model, and that the high p_\perp suppression is induced by the mismatch of the evolution speed between the proton (deuteron) and the nucleus. The nucleus is closer to saturation and evolves slower than the proton.

References

1. For a recent review, see E. Iancu and R. Venugopalan, hep-ph/0303204.
2. L. Lipatov, *Sov. J. Nucl. Phys.* **23**, 338 (1976), E. Kuraev, L. Lipatov and V. Fadin, *Sov. Phys. JETP* **45**, 199 (1977), I. Balitsky and L. Lipatov, *Sov. J. Nucl. Phys.* **28**, 822 (1978).
3. I. Balitsky, *Nucl. Phys.* **B463**, 99 (1996), Y. Kovchegov, *Phys. Rev.* **D60**, 034008 (1999).
4. S. Munier and R. Peschanski, *Phys. Rev. Lett.* **91**, 232001 (2003).
5. L. Gribov, G. Levin, and M. Ryskin, *Phys. Rept.* **100**, 1 (1983).
6. E. Iancu, K. Itakura, and L. McLerran, *Nucl. Phys.* **A708**, 327 (2002).
7. A. Mueller and D. Triantafyllopoulos, *Nucl. Phys.* **B640**, 331 (2002) 331.
8. D. Triantafyllopoulos, *Nucl. Phys.* **B648**, 293 (2003).
9. A. Mueller, *Nucl. Phys.* **A724**, 223 (2003)
10. A. Stasto, K. Golec-Biernat and J. Kwiecinski, *Phys. Rev. Lett.* **86**, 596 (2001).
11. D. Kharzeev and E. Levin, *Phys. Lett.* **B523**, 79 (2001).
12. K. Golec-Biernat and M. Wüsthoff, *Phys. Rev.* **D59**, 014017 (1999), *ibid.* **D60**, 114023 (1999).
13. E. Iancu, K. Itakura and S. Munier, *Phys. Lett.* **B590**, 199 (2004).
14. I. Arsene *et al.* [BRAHMS Collaboration], arXiv:nucl-ex/0403005.
15. D. Kharzeev, Y. Kovchegov & K. Tuchin *Phys. Rev.* **D68**, 094013 (2003).
16. J. Albacete, N. Armesto, A. Kovner, C. Salgado and U. Wiedemann, *Phys. Rev. Lett.* **92**, 082001 (2004)
17. E. Iancu, K. Itakura and D. Triantafyllopoulos, *Nucl. Phys.* **A742**, 182 (2004).